Generalized Average Model of Series - Parallel Resonant Converter with Capacitive Output Filter for High Power Application

Jean-Romain Sibue, Jean-Paul Ferrieux, Gérard Meunier, Robert Périot, Edith Clavel

Generalized Average Model of Series – Parallel Resonant Converter with Capacitive Output Filter for High Power Application.

SIBUE J.-R.[1, 2], FERRIEUX J.-P[1]., MEUNIER G.[1], PERIOT R.[2], CLAVEL E.[1]
[1]G2ELAB, ENSE3 – BP46 – 38402 Saint Martin d'Hères
[2]ALSTOM, BP4 – Rue du docteur Guinier, 65601 Séméac Cedex
jean-romain.sibue@g2elab.grenoble-inp.fr, jean-paul.ferrieux@g2elab.grenoble-inp.fr,
gerard.meunier@g2elab.grenoble-inp.fr, robert.periot@transport.alstom.com, edith.clavel@g2elab.grenoble-inp.fr

***Abstract* – This paper presents an accurate model of series parallel resonant converter with capacitive output filter. Thanks to this analytic study, it is possible to determine rapidly and easily the steady state. Furthermore a design methodology is proposed to choose series and parallel resonant frequencies in order to optimize the behavior of the converter. Simulations are used to demonstrate the accuracy and to check the design methodology.**

LIST OF ABBREVIATIONS

C_f	Output filter capacitor (F)
C_f*	Equivalent output filter capacitor (F)
C_p	Parallel resonant capacitor (F)
C_p*	Equivalent parallel resonant capacitor (F)
C_s	Series resonant capacitor (F)
d	Duty cycle full bridge output voltage (no unity)
I_D	Rectifier diode current (A)
I_{LF}	Primary current (A)
I_{LM}	Magnetizing current (A)
I_{T2}	Equivalent secondary current of transformer (A)
L_f	Leakage inductance (H)
L_m	Magnetizing inductance (H)
m	Transformer ratio (no unity)
Ψ	Rectifier non conduction angle (rad)
R	Load resistance (Ω)
R*	Equivalent load resistance (Ω)
V_{AB}	Full bridge output voltage (V)
V_{Cs}	Series resonant capacitor voltage (V)
V_{Cp}	Parallel resonant capacitor voltage (V)
V_{Cp*}	Equivalent parallel resonant capacitor voltage (V)
V_{DC}	Input DC supply voltage (V)
V_O	Output voltage, load resistance voltage (V)
V_S	Equivalent output voltage, equivalent load resistance voltage (V)
ω	Angular switching frequency (rad/s)

I. INTRODUCTION

Many studies deal with inverter driven high power magnetic devices, such as transformer with large air gap with or without magnetic cores [1], [2], [3]. This paper mainly interests in transformer loosely coupled (coupling coefficient can be equal near to 0.6) with large air gap (several centimeters) and magnetic cores in electrical vehicle application. But method and results can be applied to any system which uses series parallel resonant converter with capacitive output filter.

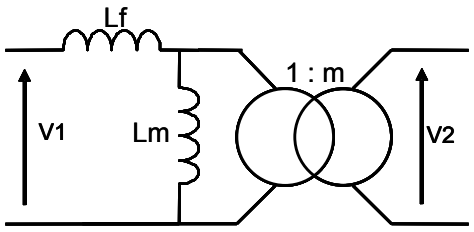

Fig. 1. Electrical model of a two windings transformer.

Loosely coupled transformer has a greatly inductive behavior. Indeed, the equivalent electrical model (Fig. 1) is composed of a small magnetizing inductance and a large leakage inductance. If this kind of transformer is supplied by a traditional full bridge, the primary current increases on account of large magnetizing current. Furthermore, the leakage inductance imposes an important voltage drop. But it is possible to add capacitors in order to compensate inductive behavior. For example, a capacitor in series with Lf compensates the voltage drop and a capacitor in parallel at the

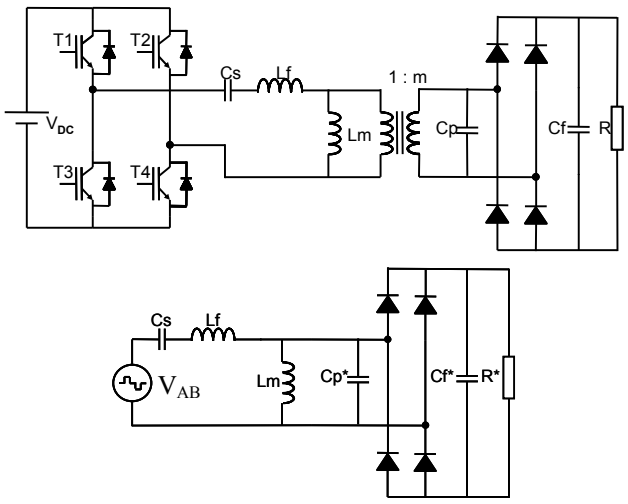

Fig. 2. Series – parallel resonant converter with capacitive output filter and equivalent scheme of the converter.

secondary can reduce the magnetizing current effect. This converter is called Series Parallel (SP) converter. Keeping voltage source at input, other solution like Series Series (SS) exists but it is not studied in this paper. Generally the desired topology is DC-DC converter. Therefore the last stage of conversion is composed of a rectifier and a filter. To win place and therefore to improve the integration, the classical filter LC is replaced by only one capacitor. The topology studied is the series parallel resonant converter with capacitive output filter (Fig. 2). Furthermore, voltage and current waveforms in components are quasi sinusoidal that reduces losses and EMC problems.

Complete steady state analyses have already been realized, but they use numerical method [4] or equivalent impedance method with iterative algorithm [5]. Otherwise some papers present a similar method for PRC-LCC resonant topology with a capacitive output filter [6], [7], [8].

This paper presents the different steps to obtain the generalized average model of this converter. Afterwards, a steady state study is presented. Eventually, a design methodology to choose series and parallel resonant frequencies in order to optimize the behavior of the converter is proposed (values of magnetizing and leakage inductances are supposed known and imposed).

II. GENERALIZED AVERAGE MODEL

A. Circuit description and general presentation

From the full scheme of the converter it is easy to deduce the equivalent scheme of Fig. 2. The DC voltage source and the full bridge are represented by a square AC voltage source of variable duty cycle and variable frequency. The components at the secondary are taken back primary. We can deduce the new values of these equivalent components from (1), (2) and (3).

$$C_{p*} = m^2 \cdot C_p \tag{1}$$

$$C_{f*} = m^2 \cdot C_f \tag{2}$$

$$R* = R/m^2 \tag{3}$$

Fig. 3 shows the main voltages and currents waveforms. When the rectifier is conducting, two voltage sources are connected in parallel (V_{Cp*} and V_S). This is possible thanks to the rectifier composed of diodes which connect the two voltage sources only when theirs potentials are equals. This has consequences on the study of the generalized average model of this converter. Indeed, this model is based on the representation in complex Fourier series. Complex coefficients are calculated from (4). It is the moving average of an harmonic of k rank.

$$\langle X \rangle_k = \frac{1}{T} \cdot \int_{t_0-T}^{t_0} X(\tau) \cdot e^{-j \cdot k \cdot \omega \cdot \tau} \cdot d\tau \tag{4}$$

All electrical magnitudes are quasi sinusoidal with no DC component and low harmonics except to voltage across the parallel capacitor. Therefore, we apply generalized average model to converter at rank one except to parallel capacitor. The fundamental property (5) of this model, widely used in this study, is deduced from (4).

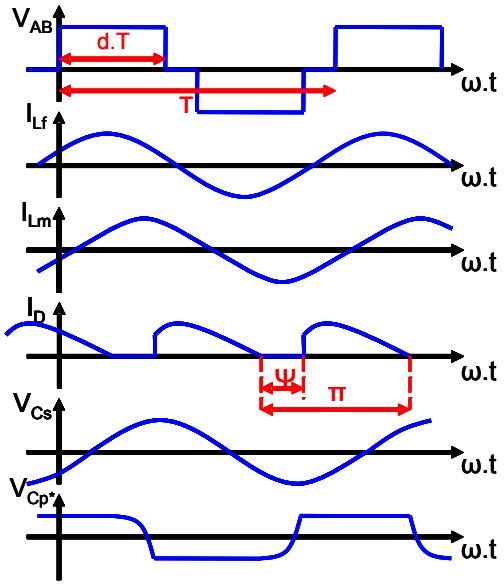

Fig. 3. Main voltages and currents waveforms.

$$\frac{d}{dt}\langle X \rangle_k = \left\langle \frac{d}{dt} X \right\rangle_k - j \cdot k \cdot \omega \cdot \langle X \rangle_k \tag{5}$$

To simplify the study of the converter, some hypotheses are made: converter is without losses, switch and diodes are ideal, and input and output DC voltage are supposed constant.

B. State variables and state equations

The first step consists to determine the state variables. This is the current for inductances and voltage for capacitors. For each state variable, we write non linear equations (6), (7), (8) and (9) except for parallel capacitor because it can not be considered like a state variable.

$$L_f \cdot \frac{d\, i_{Lf}(t)}{dt} = V_{AB}(t) - V_{Cs}(t) - V_{Cp*}(t) \tag{6}$$

$$C_s \cdot \frac{d\, V_{Cs}(t)}{dt} = i_{Lf}(t) \tag{7}$$

$$L_m \cdot \frac{d\, i_{Lm}(t)}{dt} = V_{Cp*}(t) \tag{8}$$

$$C_{f*} \cdot \frac{d\, V_s(t)}{dt} = \left| i_D(t) \right| - \frac{V_s(t)}{R*} \tag{9}$$

Afterwards, we apply (5) to equations (6)-(9). When electrical magnitudes are alternating, k is equal to one (10)-(12), otherwise it is equal to zero (13).

$$L_f \cdot \frac{d\langle i_{Lf}(t)\rangle_1}{dt} = -j \cdot L_f \cdot \omega \cdot \langle i_{Lf}(t)\rangle_1 + \langle V_{AB}(t)\rangle_1 - \langle V_{Cs}(t)\rangle_1 - \langle V_{Cp*}(t)\rangle_1 \tag{10}$$

$$C_s \cdot \frac{d\langle V_{Cs}(t)\rangle_1}{dt} = -j \cdot C_s \cdot \omega \cdot \langle V_{Cs}(t)\rangle_1 + \langle i_{Lf}(t)\rangle_1 \quad (11)$$

$$L_m \cdot \frac{d\langle i_{Lm}(t)\rangle_1}{dt} = -j \cdot L_m \cdot \omega \cdot \langle i_{Lm}(t)\rangle_1 + \langle V_{Cp*}(t)\rangle_1 \quad (12)$$

$$C_{f*} \cdot \frac{d\langle V_s(t)\rangle_0}{dt} = \langle |i_D(t)| \rangle_0 - \frac{\langle V_s(t)\rangle_0}{R*} \quad (13)$$

Equations (10)-(12) are complex. The next step consists to separate real and imaginary parts to obtain only real equations. Therefore, the complex state variables are written like a sum of a real part and an imaginary part.

$$\langle i_{Lf}(t)\rangle_1 = x1 + j \cdot x2 \quad (14)$$

$$\langle V_{Cs}(t)\rangle_1 = x3 + j \cdot x4 \quad (15)$$

$$\langle i_{Lm}(t)\rangle_1 = x5 + j \cdot x6 \quad (16)$$

$$\langle V_{Cp*}(t)\rangle_1 = x7 + j \cdot x8 \quad (17)$$

$$\langle V_s(t)\rangle_0 = x9 \quad (18)$$

Amplitude of first harmonic of electrical magnitudes is deduced from the following expression.

$$\hat{X} = 2 \cdot \sqrt{\mathrm{Re}(X)^2 + \mathrm{Im}(X)^2} \quad (19)$$

The full bridge generates a square voltage V_{AB} of duty cycle d and frequency f_{sw} that corresponding at angular frequency ω. So, the complex Fourier coefficient can be calculated from (4) with k equals to one.

$$\langle V_{AB}(t)\rangle_1 = \frac{V_{DC}}{\pi}\begin{pmatrix} \sin(2 \cdot \pi \cdot d) + \\ j \cdot (\cos(2 \cdot \pi \cdot d) - 1) \end{pmatrix} \quad (20)$$

When the rectifier is conducting, like the parallel resonant capacitor voltage is fixed, the current in this component is equal to zero. Therefore the current in the diode is equal to the equivalent secondary current (primary current minus magnetizing current). The average current in a diode of the rectifier is equal to load current. We obtained the expression (22).

$$\begin{aligned} \langle |i_D(t)| \rangle_0 &= \frac{1}{2 \cdot \pi} \cdot \int_0^{2 \cdot \pi} |I_{T2} \cdot \sin(\theta)| \cdot d\theta \\ &= \frac{1}{\pi} \cdot \int_\Psi^{\pi} I_{T2} \cdot \sin(\theta) \cdot d\theta \end{aligned} \quad (21)$$

$$\langle |i_D(t)| \rangle_0 = I_S = \frac{I_{T2} \cdot (1 + \cos(\Psi))}{\pi} \quad (22)$$

From (19) and Kirchhoff laws, we can deduce the following expression for the equivalent secondary output current:

$$I_{T2} = 2 \cdot \sqrt{(x1 - x5)^2 + (x2 - x6)^2} \quad (23)$$

In the expression (22), Ψ represents the rectifier non conduction angle. To obtain the expression of Ψ, we calculate the expression of the parallel resonant capacitor voltage when the rectifier is not conducting. We obtain the following equation:

$$\begin{aligned} V_{Cp*}(\Psi) = V_s &= -V_s + \frac{I_{T2}}{C_{p*} \cdot \omega} \cdot (1 - \cos(\Psi)) \\ \Rightarrow \; V_s = R* \cdot I_S &= \frac{I_{T2}}{2 \cdot C_{p*} \cdot \omega} \cdot (1 - \cos(\Psi)) \end{aligned} \quad (24)$$

From (22) and (24), we deduce the expression of rectifier non conduction angle:

$$\Psi = \cos^{-1}\left(\frac{\pi - 2 \cdot R* \cdot C_{p*} \cdot \omega}{\pi + 2 \cdot R* \cdot C_{p*} \cdot \omega}\right) \quad (25)$$

To obtain the final generalized average model, we separate real and imaginary parts in equations (10)-(13).

$$\begin{aligned} Lf \cdot \frac{d\,x1}{dt} &= Lf \cdot \omega \cdot x2 - x3 - x7 \\ &\quad + \frac{V_{DC}}{\pi} \cdot \sin(2 \cdot \pi \cdot DC) \end{aligned} \quad (26)$$

$$\begin{aligned} Lf \cdot \frac{d\,x2}{dt} &= -Lf \cdot \omega \cdot x1 - x4 - x8 \\ &\quad + \frac{V_{DC}}{\pi} \cdot (\cos(2 \cdot \pi \cdot DC) - 1) \end{aligned} \quad (27)$$

$$Cs \frac{d\,x3}{dt} = Cs \cdot \omega \cdot x4 + x1 \quad (28)$$

$$Cs \frac{d\,x4}{dt} = -Cs \cdot \omega \cdot x3 + x2 \quad (29)$$

$$Lm \cdot \frac{d\,x5}{dt} = Lm \cdot \omega \cdot x6 + x7 \quad (30)$$

$$Lm \cdot \frac{d\,x6}{dt} = -Lm \cdot \omega \cdot x5 + x8 \quad (31)$$

$$\begin{aligned} Cf* \cdot \frac{d\,x9}{dt} &= \frac{2 \cdot \sqrt{(x1 - x5)^2 + (x2 - x4)^2}}{\pi} \\ &\quad \cdot (1 + \cos(\Psi)) - \frac{1}{R*} \cdot x9 \end{aligned} \quad (32)$$

The system of equation (26)-(32) contains more unknowns than equations. The two extra unknowns are x7 and x8 that corresponds to parallel resonant capacitor voltage.

C. Calculus of x7 and x8

Like parallel resonant capacitor voltage is clamped to output voltage when the rectifier is conducting, it is not possible to use generalized average model to determine this voltage. It is necessary to express x7 and x8 in function of other real state variables and converter's characteristics. Therefore, the first complex Fourier coefficient of parallel resonant capacitor voltage (33) and equivalent secondary current of the transformer (34) are calculated. Afterwards, the complex equivalent impedance is deduced [5].

$$V_{Cp^*(1)} = \frac{I_{T2(1)}}{2 \cdot \pi \cdot C_{p^*} \cdot \omega} \cdot \begin{pmatrix} \sin(\Psi) \cdot \cos(\Psi) \\ -\Psi - j \cdot \sin^2(\Psi) \end{pmatrix} \quad (33)$$

$$I_{T2(1)} = \frac{-j \cdot I_{T2}}{2} \quad (34)$$

$$x7 + j \cdot x8 = \frac{V_{Cp^*(1)}}{I_{T2(1)}} \cdot I_{T2} \Leftrightarrow x7 + j \cdot x8 = Z_{Cp^*} \cdot \left((x1 - x5) + j \cdot (x2 - x6) \right) \quad (35)$$

Finally, from (35) separating real and imaginary parts, the two following expressions are obtained [6], [8]:

$$x7 = K \cdot \left(\sin^2(\Psi) \cdot (x1 - x5) + \mu \cdot (x2 - x6) \right) \quad (36)$$

$$x8 = K \cdot \left(\sin^2(\Psi) \cdot (x2 - x6) - \mu \cdot (x1 - x5) \right) \quad (37)$$

$$K = \frac{1}{\pi \cdot m^2 \cdot Cp \cdot \omega} \quad (38)$$

$$\mu = \Psi - \sin(\Psi) \cdot \cos(\Psi) \quad (39)$$

The system is linear because all equations are independent and they only depend on converter characteristics. Therefore, from state matrix we can easily obtain the steady state solution.

III. STEADY STATE STUDY

To obtain the steady state solution, the derivatives in equations (26)-(32) are considered constant and equal to zero. The solution of the system is showed in (43). To limit the size of the state matrix (42), the system has been simplified. The state vector (40) contains four real state variables. Others sate variables are deduced from state vector X.

$$X = \begin{bmatrix} x1 & x2 & x5 & x6 \end{bmatrix}^T \quad (40)$$

$$Y = -\frac{V_{DC}}{\pi} \cdot \begin{bmatrix} \sin(2 \cdot \pi \cdot d) & (\cos(2 \cdot \pi \cdot d) - 1) & 0 & 0 \end{bmatrix}^T \quad (41)$$

$$A = \begin{bmatrix} -K \cdot \sin^2(\Psi) & Lf \cdot \omega - \frac{1}{Cs \cdot \omega} - K \cdot \mu & K \cdot \sin^2(\Psi) & K \cdot \mu \\ -Lf \cdot \omega + \frac{1}{Cs \cdot \omega} + K \cdot \mu & -K \cdot \sin^2(\Psi) & -K \cdot \mu & K \cdot \sin^2(\Psi) \\ -K \cdot \mu & K \cdot \sin^2(\Psi) & -Lm \cdot \omega + K \cdot \mu & -K \cdot \sin^2(\Psi) \\ K \cdot \sin^2(\Psi) & K \cdot \mu & -K \cdot \sin^2(\Psi) & Lm \cdot \omega - K \cdot \mu \end{bmatrix} \quad (42)$$

$$Y = A \cdot X \Leftrightarrow X = A^{-1} \cdot Y \quad (43)$$

Output voltage is deduced from (44).

$$Vo = \frac{4 \cdot R \cdot \sqrt{(x_1 - x_5)^2 + (x_2 - x_6)^2}}{(\pi + 2 \cdot R \cdot Cp \cdot \omega) \cdot m} \quad (44)$$

Table 1 shows the characteristics of converter chosen to demonstrate the accuracy of the generalized average model. The values of series and parallel capacitors have been chosen such as resonant frequencies have been equal to 25 kHz.

TABLE I
VALUE OF DIFFERENTS COMPONENTS

Abbreviation	Value
V_{DC}	750 V
Cs	22.6 µF
Lf	1.8 µH
Lm	3 µH
m	3.789 (no unity)
Cp	0.9 µF
Cf	1 mF
R	5 Ω

The generalized average model has been implemented in MATLAB® function and theoretical results have been compared to simulations realized with PSIM®. Fig. 4 shows the output voltage versus switching frequency. The duty cycle is equal to 50 %. The resonant frequency of converter is around 32 kHz whereas series and parallel resonant frequencies are equal to 25 kHz.

The more the switching frequency is close to series resonant frequency, the more waveforms are sinusoidal. Like genralized average model is based on the study of first harmonic, this justifies the accuracy of the model around 25 kHz. When switching frequency increases the relative difference is low, whereas for low switching frequency, the accuracy is poor on account of large harmonic distorsion rate in comparison to fundamental. Indeed for primary current, it is of 57 % at 15 kHz, whereas it is of 11 % at 35 kHz. From 22 kHz to 40 kHz, the relative difference between theory and simulation does not exceed 5 %.

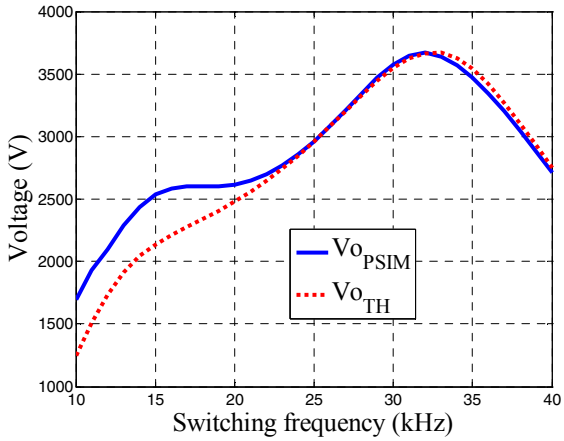

Fig. 4. Output voltage versus switching frequency with series and parallel resonant frequencies equal to 25 kHz.

Another control mode is possible. Indeed the switching frequency can be fixed and the duty cycle is variable. The study was realized with two switching frequency (25 kHz and 32 kHz) and the duty cycle fluctuates from 5 % to 50 %. The relative difference does not exceed 8 %. The more the duty cycle is small, the more the relative difference is large. This technique of control is attractive because it is possible to always operate at the desired switching frequency.

For series parallel resonant converter with output capacitive filter it is better to have a switching frequency higher than series resonant frequency in order to keep quasi sinusoidal waveforms in power component in order to limit losses.

In part three, series and parallel resonant frequencies have been imposed. Now, the aim is to find a design methodology to choose these two frequencies which are adjustment parameters of this converter.

IV. ADJUSTMENT OF SERIES AND PARALLEL RESONANT FREQUENCIES

For this study, the values of magnetizing and leakage inductances are supposed known and imposed. Therefore, adjust series and parallel resonant frequencies consist to determine the values of series and parallel capacitors (45), (46).

$$C_S = \frac{1}{4 \cdot \pi^2 \cdot f_{ress}{}^2 \cdot L_f} \tag{45}$$

$$C_p = \frac{1}{m^2 \cdot 4 \cdot \pi^2 \cdot f_{resp}{}^2 \cdot L_m} \tag{46}$$

To adjust these frequencies it has been chosen to study output characteristics of converter.

A. Adjustment of series resonant frequency

Series resonant frequency has more effects on output characteristic than parallel resonant frequency. Therefore to adjust these frequencies, the first step consists to determine the series resonant frequency.

Fig. 5 shows output characteristics for different switching frequencies from 20 kHz to 32 kHz. Series and parallel resonant frequencies are always equal to 25 kHz. The best output characteristic is obtained for a switching frequency of 26 kHz. Indeed the charge variation is important whereas output voltage is quasi constant. Furthermore, the third harmonic of primary current is very low that limits losses.

Therefore to determine series resonant frequency, we choose an arbitrary ratio β smaller than one between series resonant frequency and switching resonant frequency. Usually the switching frequency is imposed, so series resonant frequency is deduced from switching frequency (47).

$$f_{ress} = \beta \cdot f_{sw} \tag{47}$$

A reasonable value of β is around 0.95.

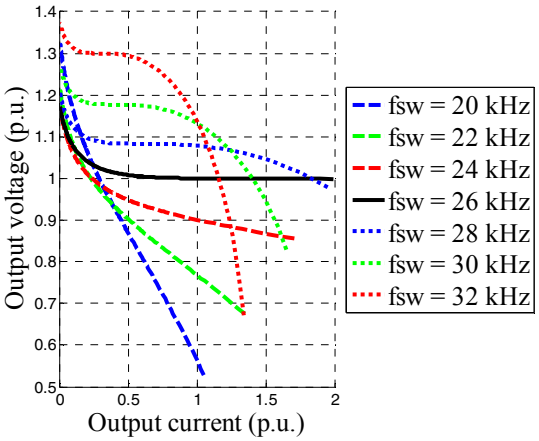

Fig. 5. Normalized output characteristics for different switching frequencies from 20 kHz to 32 kHz with series and parallel resonant frequencies equal to 25 kHz.

B. Adjustment of parallel resonant frequency

Now, series resonant and switching frequencies are imposed and known. They are respectively equal to 25 kHz and 26 kHz. Fig. 6 shows output characteristics for different parallel resonant frequency from 20 kHz to 40 kHz.

Fig. 6 does not give adjustment condition for parallel resonant frequency except to adjust of output voltage. But to use parallel resonant frequency to obtain desired gain does not allow to take maximum benefits from this topology because the reactive energy of parallel tank is not compensated. Input voltage source has to provide this energy and therefore primary current increases. Therefore we are free in the choice of parallel resonant frequency to minimize primary current if we are able to adjust voltage gain of converter with turn ratio of transformer or input voltage. We can notice (Fig. 6) output voltage variation is quasi independent of parallel resonant frequency.

The aim is to minimize primary current and therefore the over sizing of full bridge. We do not interest in rectifier

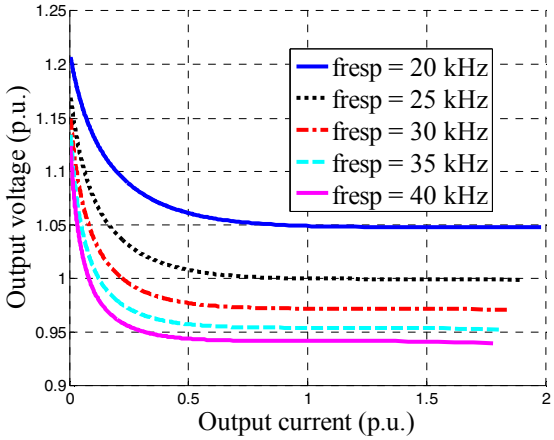

Fig. 6. Normalized output characteristics for different parallel resonant frequencies from 20 kHz to 40 kHz with series resonant frequencies equal to 25 kHz and switching frequency equal to 26 kHz.

because it only transmits active power. It is the same thing for capacitors. For example, for parallel resonant capacitor, there is no current if its equivalent impedance is very high, that corresponds to parallel resonant frequency very high. But in this case the converter becomes only a series resonant converter. So, the aim is to minimize the full bridge kW/kVA rating. Like the converter is supposed without losses, the expression of kW/kVA rating can be written:

$$\frac{P}{S} = \frac{\frac{Vo^2}{R}}{V_{ABrms} \cdot I_{Lfrms}} = \frac{Vo^2}{R \cdot V_{ABrms} \cdot I_{Lfrms}} \qquad (48)$$

Fig. 7 shows the theoretical and PSIM® simulation results of kW/kVA rating versus parallel resonant frequency. Curve 1 is calculated from true voltage of first harmonic of full bridge output voltage (49) from equations (19) and (20). Curve 3 is calculated from true full bridge output voltage (50).

$$V_{ABrms\,(1)} = \frac{2 \cdot \sqrt{1 - \cos(2 \cdot \pi \cdot d)}}{\pi} \cdot V_{DC} \qquad (49)$$

$$V_{ABrms} = \sqrt{2 \cdot d} \cdot V_{DC} \qquad (50)$$

The waveforms are similar and the relative difference between curve 1 and 2 is around 10 % whereas maximum relative difference between curves 2 and 3 is only of 1 %. To analyze this, the logarithmic derivative (51) from (48) is calculated. From this expression, we deduce the maximum relative difference (20 %) which justifies error between curves 1 and 2. Curve 3 highlights that error comes from calculus of true value of full bridge output voltage which is a square voltage with a large harmonic distorsion rate in comparison to fundamental. By taking the expression (50) for true full bridge output voltage instead (49), accuracy is ecxellent.

$$\frac{d(P/S)}{P/S} = 2 \cdot \frac{dVo}{Vo} - \frac{dR}{R} - \frac{dV_{ABrms}}{V_{ABrms}} - \frac{dI_{Lfrms}}{I_{Lfrms}} \qquad (51)$$

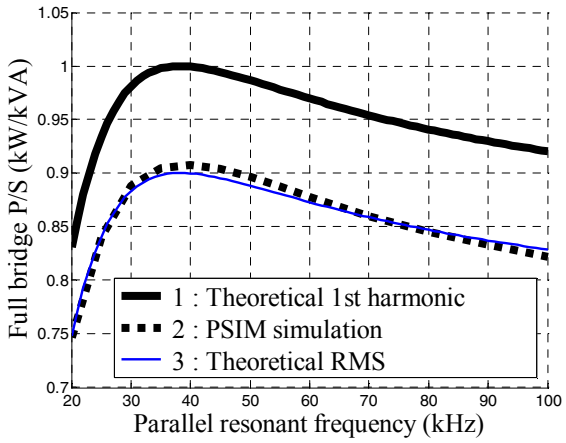

Fig. 7. Full bridge kW/kVA rating versus parallel resonant frequency with series resonant frequencies equal to 25 kHz and switching frequency equal to 26 kHz.

Like waveforms are similar and their maximums correspond to the same parallel resonant frequency, we can use the analytic model to determine the frequency which minimize the over sizing of full bridge components. In this case, the parallel resonant frequency chosen is around 40 kHz.

V. CONCLUSION

Using generalized average method, a simple analytic model has been deduced for series parallel resonant converter with capacitive output filter. From this model, it is very easy and quick to know electrical magnitudes with an excellent accuracy. Furthermore a design methodology is proposed to adjust series and parallel resonant frequencies.

Like magnetizing current and leakage inductance voltage can not be neglected at the time of design of a transformer with large air gap with or without magnetic cores, such model is very useful. Indeed, without using long simulation, it is possible to adjust resonant frequencies and to know electrical magnitudes like primary and secondary current in order to take into account these magnitudes in the design methodology of this kind of transformer.

This paper does not present experimental results because global aim is to design a transformer with large air gap considering influence of such a converter. Currently, proposed model and adjustment of resonant frequencies have been implemented in designing algorithm of transformer.

REFERENCES

[1] K. D. Papastergiou, D. E. Macpherson "An airborne radar power supply with contactless transfer of energy – Part I: Rotating transformer," *IEEE Trans. Ind. Electron.,* vol. 54, pp. 2874-2884, October 2007.

[2] C.-S. Wang, O. H. Stielau, G. A. Govic, "Design considerations for a contactless electric vehicle battery charger", *IEEE Trans. Ind. Electron.,* vol. 52, pp. 1308-1314, October 2005.

[3] J. Sallan, J. L. Villa, A. Llombart, J. F. Sanz, "Optimal design of ICPT systems applied to electric vehicle battery charge", *IEEE Trans. Ind. Electron.,* vol. 56, pp. 2140-2149, June 2009.

[4] R. Laouamer, J.-P. Ferrieux, and H. Benqassmi, "A comparison of resonant converter topologies with three and four energy storage elements for automatic inductive charging applications," *Electric Machines and Power Systems*, Vol. 27, pp. 221–236, 1999.

[5] Y. A. Ang, C. M. Bingham, M.P. Foster, D.A. Stone, D. Howe, "Design oriented analysis of fourth order LCLC converters with capacitive output filter", *IEEE Proc. Electro. Power Appl.,* vol. 152, no. 2, pp. 310-322, March 2005.

[6] J. A. Martin-Ramos, J. Diaz, A. M. Pernia, J. M. Lopera, F. Nuno, "Dynamic and steady-state models for the PRC-LCC resonant topology with a capacitor as output filter", *IEEE Trans. Ind. Electron.,* vol. 54, no. 4, pp. 2262-2275, August 2007.

[7] J. A. Martin-Ramos, A. M. Pernia, J. Diaz, F. Nuno, J. M. Alonso, "A circuit for the large and small signal dynamic modeling of the PRC-LCC resonant topology with a capacitor as output filter", *in Proc. IEEE PESC 2005,* pp. 635-641.

[8] J. A. Martin-Ramos, , J. Diaz , A. M. Pernia, F. Nuno, J. Sebastian, "A large signal model for the PRC-LCC topology with a capacitor as output filter", *in Proc. IEEE APEC 2002,* pp. 1120-1126.